City Form Lab

at SUTD, established in collaboration with MIT | **cityform.mit.edu**

Working Paper

Unpublished, in press, or in review.

Geometrical solution space for grid structures with double-walled edges

Andres Sevtsuk

Singapore University of Technology and Design

Raul Kalvo

Singapore University of Technology and Design

Abstract. *This paper introduces a method for creating double-curved grid structures made out of flat components, where fabrication is limited to only 2-dimensional cutting, making complex architectural structures accessible to a wider audience at a lower cost. The focus of the paper is to identify the limitations and to map the geometric solution-space of the method for real world construction applications. A double-walled nature of the structure enables us to significantly reduce the geometric complexity of the grid structure's nodes – instead of needing to find a combined geometric intersection for all edges meeting at a node, our solution instead requires determining a pair of adjacent planes at a time, as many times as a node's degree. But if any of these pairs of planes around a node is torsioned relative to the node's normal, then collisions might occur between different pairs of planes. This paper discusses the geometric solution-space under which such collisions are avoided, making the structural joints easy to build. As a proof of concept, we demonstrate the use of this method in a design-build pavilion that was realized at the Singapore University of Technology and Design in 2013.*

Introduction

Grid structures are part of a larger family of thin-shell structures that have a long history of structural investigations [Mungan and Abel. 2012], [Schlaich 2002]. Along with funicular vaults, monoliths and membrane shells, their effective structural properties have made grid structures attractive for constructing bridges, hangars, domes, and pavilions that require uninterrupted covered space. Grid structures save material by using double-curved forms that follow the lines of structural thrust, thereby achieving economical, efficient and elegant structures. The geometric forms of membrane and funicular shell structures are dictated by the distribution of forces, where tensile structures work fully in tension and funicular shells fully in compression. Whereas tensile structures almost always form anticlastic surfaces [Pronk and Diminicus 2013], with exception of pneumatic shells, which are synclastic, funicular shells form dominantly synclastic surfaces.

Grid structures and monolithic shells provide much more freedom since they can combine tension and compression into one surface. A double curved geometrical aspect can give grid structures more global stability and reduce material usage in comparison to structures that work predominantly in bending (e.g. wall-ceiling or column-beam structure).

This paper discusses a method that allows grid structures to be constructed from a curved line network that may be regular or irregular using arbitrary n-gons while keeping all structural elements planar, allowing them to be fully fabricated on 2D cutting machines. The details of this method are discussed in [Sevtsuk and Kalvo 2014]. The key benefit of the approach is that it offers great freedom in form and in the structural line-network design, while assuring that all joints and beams can be fabricated economically from two-dimensional sheet material. An additional benefit is that the structure can be entirely prefabricated and assembled in modular components on site without large space constraints and without high-precision work on site.

The geometric construction of the discussed system requires two key conditions. First, the structure needs to be composed of two parallel walls around each network edge, and second, the adjoining non-parallel walls need to be extruded at particular angles, such that straight intersection lines are achieved on the interior planes of walls. Both conditions are necessary to guarantee 2D fabrication.

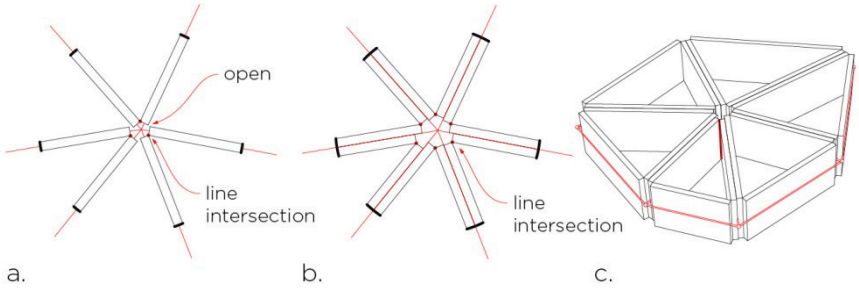

Figure 1. Left: The proposed method is not feasible with single-walls on free-form line networks without creating gaps between neighboring elements or modifying the input line network. Middle and Right: A continuous grid structure is achieved through double-walls around each network edge, where the planes are extruded at such angles that straight intersection lines are achieved between all interior planes meeting around a node.

Figure 1 shows in plan and axonometric how a continuous grid structure is achieved through double walls around each network edge, where the planes are extruded at such angles that straight intersection lines are achieved within all interior planes meeting around a node (Figure 2). In the case of a single-walled solution (left), the pairs of panels on the left and right of the node cannot move any closer to the node along their own axes without starting to intersect. The single-walled solution therefore does not allow us to achieve straight intersection lines between all adjacent panels around a node, which in turn inhibits the possibility of flat-bed cutting.

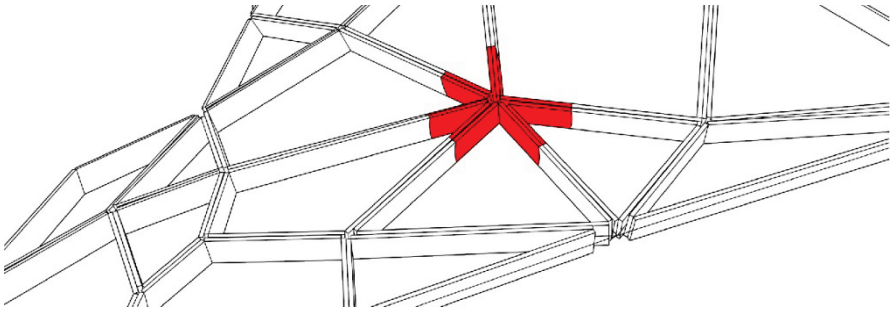

Figure 2. A typical node in a grid structures with double-walled edges.

The joints can be connected along a linear intersection line between two neighboring planes of grid structure's beams through a linear fastener (e.g. weld, fold, hinge etc.). These intersection lines are marked as loop-node vectors ($\upsilon_{l,n}$) in Figure 3. The figure also introduces other notations used throughout the paper. The vertical depth of the walls becomes a structural variable that can be increased for stronger linear connections. Gaps can be formed between two parallel panels along each network edge using spacer blocks. The material thickness of the panels as well as these gaps can be useful for avoiding collisions between different panels around joints, as discussed below. The proposed solution allows a wide variety of curved line networks to be turned into a grid structures in an economical and highly flexible way.

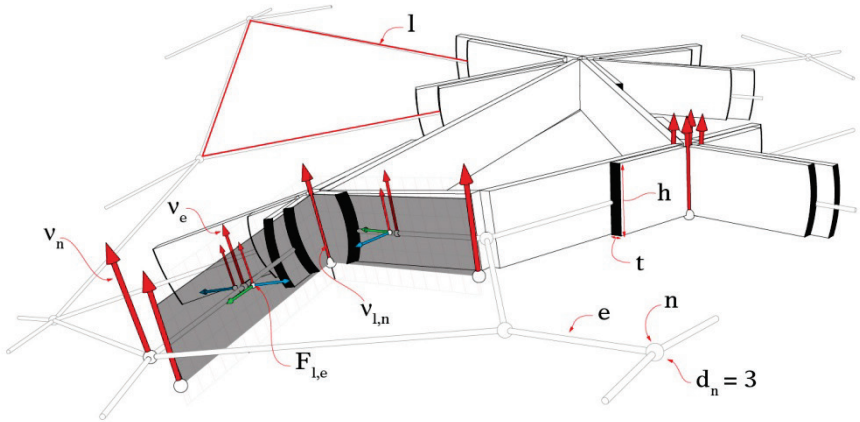

Figure 3. Geometrical notations used: Node (n), Node degree (d_n), Node vector (υ_n), Edge (e), Edge vector (υ_e), Loop (l), Loop-node vector ($\upsilon_{l,n}$), Loop-edge frame ($F_{l,e}$). Panel height (h). Panel thickness (t)

2 Solution space

The proposed grid structures are composed of beams with double walls along edges and a series of nodes that act as joints between different beams. The solution space of our geometric framework is the universe of geometric parameters and material dimensions under which no panels of the grid structure collide around joints. The solution space is violated when panels around node start colliding with each other, making the joints impossible to assemble (Figure 2). Collisions can appear for a number of reasons when a complex shape of the grid structure produces complex edge conditions around nodes (Figure 4). It is thus important to investigating the solution space of the proposed method for two reason. First, it is useful to know what geometric factors are causing collisions between panels at joints? And second, how can geometric parameters and material dimensions be altered to avoid collisions from occurring?

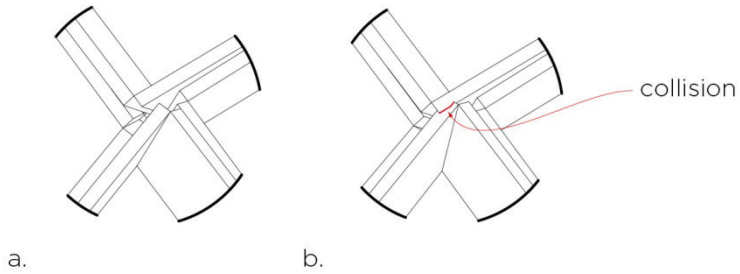

Figure 4. a. Node condition without collision. b. Node condition with collision, marked with a red line. Parameters

To find a solution space for the whole network (mesh) we start by focusing on a single node, since nodes can be solved almost independently from one another in the larger structure. All nodes can be described mathematically with a handful of variables, which cover all possible geometrical conditions (Figure 5).

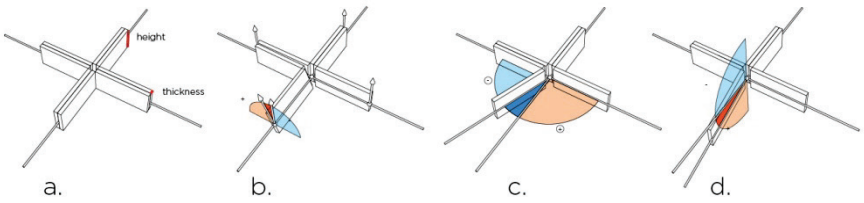

Figure 5. a. Base case of a node with degree "4", which means that 4 edges are connected to one node. In (a) none of the edges connected to the base case exhibit torsion, angle deviation or curvature. b. One of the edges contains torsion. c. One of the edge contains angular deviation. d. One of the edges contains curvature.

These variables include: a ratio between panel thickness and height (a), torsion (b), angle deviation (c), and curvature (d). Since torsion, angle deviation and curvature depend on the node's degree d_n we can collect all of them into tuples [Schneider and Eberly 2003]. A node with a degree "three" has a torsion tuple t_n with components describing torsion τ_e for every edge:

$$t_n = (\tau_1, \cdots \tau_i, \cdots \tau_e)$$

We can apply the same idea to an angle deviation tuple a_n and its components α_e, and to the curvature tuple k_n and its components κ_e. We use φ to describe the ratio between panel thickness and height (Figure 7, Figure 3). As long as the thickness-to-height ratio is constant, we can ignore the individual height and thickness values when studying the geometry around a node.

For nodes of any degree, there are three times as many variables as the node's degree plus one for the thickness-to-height ratio φ. In case of a node of degree "3" we have 10 variables, all of which can produce an effect on panel collisions. For higher degree nodes the number of variables increased exponentially and there are too many variables to test individually. But for practical purposes, heuristics can be used to eliminate configurations that do not occur in realistic construction dimensions. First, we may reduce the number of node degrees that need to be explored, since only a few degrees are commonly found in regular tessellations or mesh structures. There are three different regular tessellations – squares, regular hexagons and equilateral triangles – which respectively produce node degrees "3", "4" and "6" [Wells 1991]. However, since pentagonal tessellations can also be found in architectural use, we complete the list by adding a node with degree "5".

The next heuristic simplification comes from the tuples: t_n, a_n, k_n. An exploratory study showed that if we only changed components in one tuple at a time, keeping the others constant at the base case-case, then only the torsion components t_n caused changes in the loop node vectors $v_{l,n}$ (See Figures 3 and 6), which can potentially cause collisions.

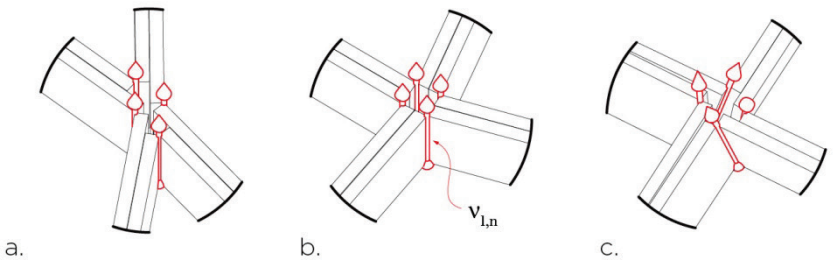

Figure 6. a. Changeing values in a_n do not change $v_{l,n}$. b. Changeing values in c_n do not change $v_{l,n}$. c. Changeing values in t_n change $v_{l,n}$.

Angle and curvature between panels are still important in combination with torsion, but we can start by investigating collisions caused by torsion in the

members. First, we need to find some realistic values for the panel thickness-to-height ratio φ, since the occurrence of collisions is linearly related to this value (as we shall demonstrate below). A base case value of $\varphi = 0.05$ corresponds in physical reality to a 12 mm thick plywood panel with a height of 240 mm. The same φ also corresponds to a 5 mm thick composite aluminum panel with a height of 100mm or a 50mm concrete panel with a 1000mm height. Figure 7 illustrates different wall thicknesses. Larger panel thickness-to-height ratios (c) tend to avoid collisions and smaller ratios (a) are more prone to collisions.

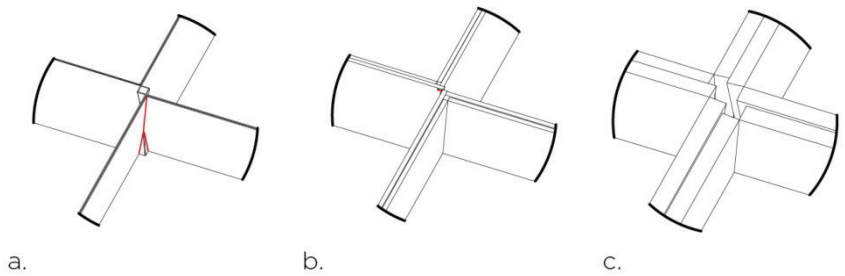

Figure 7. Keeping $t_n = (6°, -6°, 6°, -6°)$ constant and changeing $\varphi = (0.01, 0.05, 0.2)$ we see that smaller φ values produce collisions in configurations (a) and (b) (marked with red).

The first important, albeit intuitive, finding is that the simplest way to avoid collisions is to increase the panel thickness. This can be achieved by either using a thicker building material (e.g. 16mm plywood instead of 12mm) or by placing a spacer-block between two edges. Note that each pair of panels that are joined around a node share an intersection line on the inside of the loop, facing away from the node, as shown in Figure 6. Each of the panels in a double-walled edge has a material thickness that can range from close to zero (e.g. a sheet of paper) to several centimeters (e.g. a concrete panel). Depending on the panel thickness, these intersection lines can start moving outward from the node, which reduces the hazard of collisions between different panels around the node. The outward offset is furter extended if gaps are formed between the parallel panels. Manipulating panel thickness and the thickness of the spacer blocks between parallel panels can allow many curvatures and patterns of grid structures to be achieved collision-free (Figure 8).

Figure 8. A complex shape and pattern of a grid structure is achieved with no collisions between panels around nodes by taking advantage of panel thickness and spacer gaps between parallel panels.

Having chosen a base value for φ and a node degree $d_n = 4$, we are ready to explore the effects of torsion on panel collisions. To do so, we automated the generation of t_n on a computer and tested a total 6,561 different combinations of torsion on panel collisions, using

$$t_n = (\tau_1, \tau_2, \tau_3, \tau_4), \text{ where } \tau_i \in (-8°, -6°, -4°, -2°, 0°, 2°, 4°, 6°, 8°)$$

We recorded each test in a table, where the first column showed if collision occurred and the next four columns showed the combinations of torsion in the four panels. Each time a collision was observed, we recorded the maximum magnitude in torsion among all four edges as well as the directionality of the torsion in each edge. For example, a torsion combination $(-8, 2,6, -2) \xrightarrow{yields} -8$ *or* $(-6, 2,2,8) \xrightarrow{yields} 8$). For each maximum torsion indicator, we determined the percentage of tests that resulted in a collision-free node out of the total 6,561 tests. These results are shown in Figure 9 (Left). Plotting these results revealed a few important observations.

First, if τ_{max} is small enough (typically $-2 < \tau_{max} < 2$), then no collisions occur. This was expected – small torsion values do not create collisions between panels.

Second, for any given value of τ_{max}, there is no combination of $|\tau_i| < |\tau_{max}|$ where a collision occurs. That is, collisions are always predicted by the highest

absolute torsion value among all edges around a node and we do not need to keep track of the remaining lower values to detect a collision. This is important since we can now reduce the search space significantly, testing only the $t_n = (\cdots \pm|\tau_{\max,i}| \cdots)$ values. In order to make sure there is no collision for a value $|\tau_{\max}| = x$, we need to test 2^{d_n} combinations for one φ. For instance, for a node with degree "5", we need to test $2^5 = 32$ combinations. That said, it is possible to additionally use necklace combinatorics [Pólya 1937], which can reduce required combinations even further. In case of node degree "5", only 8 unique combinations are required[1].

Third, if we limit combinations so that all components in $\mathrm{t_n}$ are either positive or negative, then no collisions are found. Figure 10 shows different spiral configurations achieved through torsion around a node. Collisions are avoided regardless of particular τ values, as long as they are all either positive or negative. This seems visually logical. To confirm this, we also conducted a series of tests with $\mathrm{t_n} = (\tau_1, \tau_2, \tau_3, \tau_4)$, where $\tau_i \in (-30°, -25°, -20°, 20°, 25°, 30°)$. Taken by the maximum absolute torsion value alone, such large τ angles led to a lot of intersections (Figure 9 right side, black curve), though some positive results were also found. However, when including only combinations where all τ values have the same sign, no collisions could be found at all.

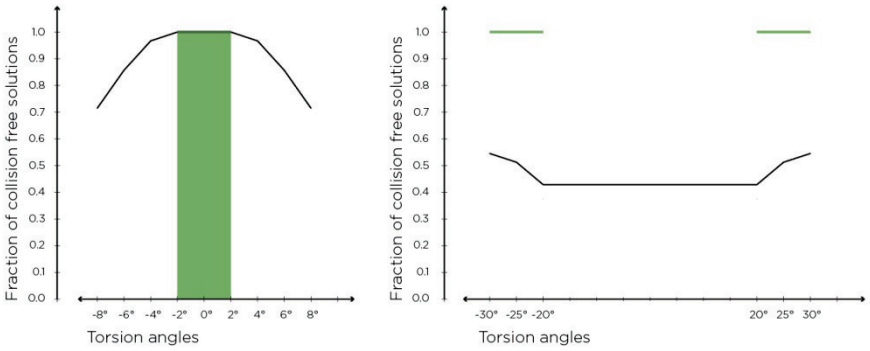

Figure 9. Left: Collision simulation results for torsion. The horizontal axis denotes the maximum magnitude of torsion values among all four edges (positive and negative) and the vertical axis shows the percentage of cases where no collisions where found under such conditions. Right: Lower graph shows the same test for larger torsion magnitudes. The upper green lines illustrate no-collision cases with large torsion angles where all edges are torsioned in the same direction

[1] Necklace combinatorics examines combinations in a continuous loop. For instance, combinations [a,a,b], [a,b,a], [b,a,a] are considered the same, since viewed in a continuous loop, the set does not have a start or end point.

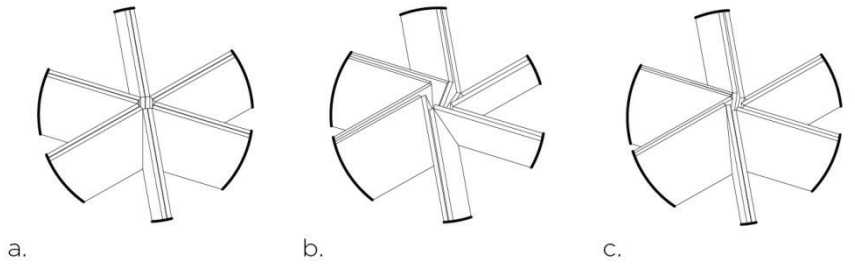

Figure 10. a. No sipiral. b. Constant spiral. c. Varibale spiral.

We learned from the previous tests that there are some values of $\tau_{\max}$ which determine whether a node with t_n faces collisions or not. We also know that this value depends on the material width-to-height ratio φ. Next, we explored the relationship between the maximum collision-free τ for different node degrees and φ ratios. In case of node degree 4, we determined the maximum τ for φ values from 0.01 to 0.23, with a test step size of 0.01 (Figure 12a). We stopped the tests around φ =0.23, since beyond this dimension, thickness-to-height ratios appear unrealistic for real-world construction – panels whose thicknesses forms a quarter of their height or more. The results are plotted in Figure 11, where different color graphs represent nodes of degree 4, 5 and 6 respectively and the different lines in the same graph illustrate the results for different combinations of τ. The lines named "$[-\tau, \tau]$" describe edge torsion combinations that contain both positive and negative torsion around a node, which is generally the most likely case for collisions to occur. We also conducted the same test for torsion combinations where the maximum negative value is half the maximum positive value – that is torsion combinations that also contain opposite directions, but less sever, illustrated with graph lines "$[-\tau/2, \tau]$". The third range of tests was limited to cases where edge torsions range only between 0 and positive or 0 and negative numbers, illustrated by the "$[0, \tau]$" curves. Recall that the remaining uniformly negative and uniformly positive torsion cases produced no collisions.

These tests revealed that there is a linear relationship in the most collision-prone cases between φ and torsion combinations with opposite signs (positive-negative). The trajectory of this relationship is important because it tells us that if we keep all torsion values less than the corresponding maximum absolute torsion value on the y-axis, then we can guarantee that no collisions occur, even under positive-negative torsion combinations. We denote the torsion values along this curve with $\tau_{f,\varphi}$, whose magnitudes are always positive. The value of $\tau_{f,\varphi}$ changes with φ. In other words, the collision-free maximum absolute torsion value depends on a material's thickness-to-height ratio. For example, $\tau_{f,0.05} = 2.85°$, $\tau_{f,0.01} = 0.55°, \tau_{f,0.1} = 5.65°$ and $\tau_{f,0.2} = 11.1°$.

Another important constant for different material thickness-to-height ratios is $\tau_{0,\varphi}$ (see the "$[0, \tau]$" curves in Figure 11). If values for a particular material

thickness-to-height ratio are higher than this curve, then torsion angles have to be either all positive or all negative in order to avoid collisions. There is also an operational range $\tau_{r,\varphi}$ which represents the overall limit to collision-free nodes. The proposed grid structure solution cannot handle edge torsion of 90° for instance. But in most common applications, the necessary edge torsion combinations remain well below 40° or 50°. At 50°, two adjacent edges can have a 100° difference in torsion.

Figure 13 presents a general overview of the solutions space with respect to edge torsion. As long as all torsion angles fall within the green zone in the chart, there are no collision in the node caused by torsion. However, collisions can still occur when torsion is combined with non-zero edge angles (a_n) or curvature (k_n). The orange zone can contain collision-free combinations, but it is important to pay attentions to the directionality of different edges torsions there, as described below. For torsion values that fall into the gray zone, a collision is guaranteed. In order to illustrate this with an example, consider a node with four edges whose respective torsion values are $\mathrm{t_n} = (2,0,0,-0.01)$ and the relationship between material thickness-to-height ratio and maximum edge torsion is $\tau_{0,\varphi} = 1.9$. Based on the $\tau_{0,\varphi} = 1.9$ value, we know that this node will produce a collision, since its maximum torsion angle is above 1.9 and the node contains both positive and negative torsion (it falls in the gray zone in Figure 13). However, if the node's torsion angles were adjusted to $\mathrm{t_n} = (1.8,0,0,-0.01)$, then the node might or might not contain collisions (it would fall in the orange zone). Whether or not there actually are collisions in this case, depends on the directionality of the edge torsions, as explained below. We should also note that if torsion angles are combined with curvature, then the gray area of Figure 13 can also yield collision-free solutions.

We conducted the same type of calculations for node degrees 4, 5, 6 and found that $\tau_{f,\varphi}$ is very similar, practically the same, for different node degrees. The lowest lines in the middle and right side graphs in Figure 12b, which illustrate the cases for 5 and 6 degree nodes respectively, demonstrate that node degree has no impact on torsion-based collisions with different material thickness-to-height ratios as long as the absolute values of torsion fall within the $\tau_{f,\varphi}$ range. That is, the same maximum torsion degree applies regardless of whether a node has 4, 5 or six edges. Note that we have left out collision tests for nodes with degree 3 – e.g. hexagonal tessellations where three edges meet at each node – since degree 3 nodes do not create any collisions anyhow.[2]

[2] In order to see this, let us look at a node in a hexagonal tessellation as surrounded by three sectors or three loops. Since each sector shares an edge with the remaining two neighboring sectors via a double wall, no collisions are possible with the neighboring walls. At least four sectors are needed for panels to start colliding.

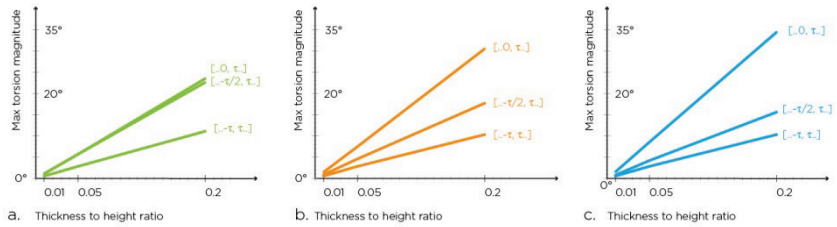

Figure 11. Graphs a, b, c show the relationship between panel thickness-to-height ratios (x-axis) and maximum torsion angle (y-axis) for different node degrees 4,5 and 6, which are marked as green (a), orange (b) and blue (c) respectively.

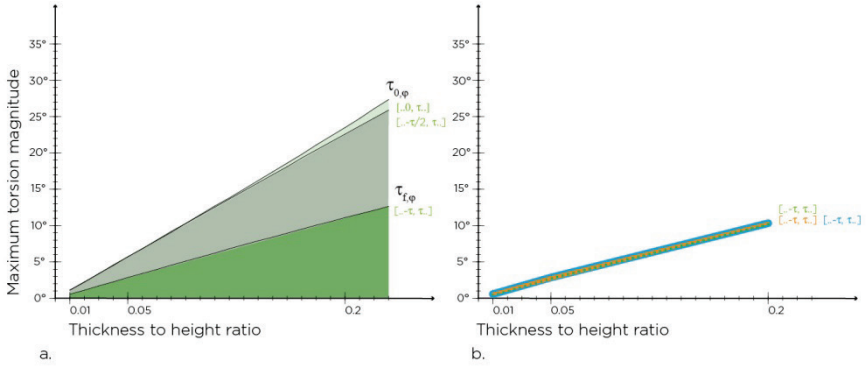

Figure 12. Graph a. shows collision-free solution spaces between maximum torsion angles and material thickness-to-height ratios in a node degree 3. The three lines descirbe maximum torsion angles for different patterns of torsion in edges around a node. Data is sampled at every 0.01 thickness-to-height ratios. Graph b shows that node degree do not have effect on $\tau_{f,\varphi}$

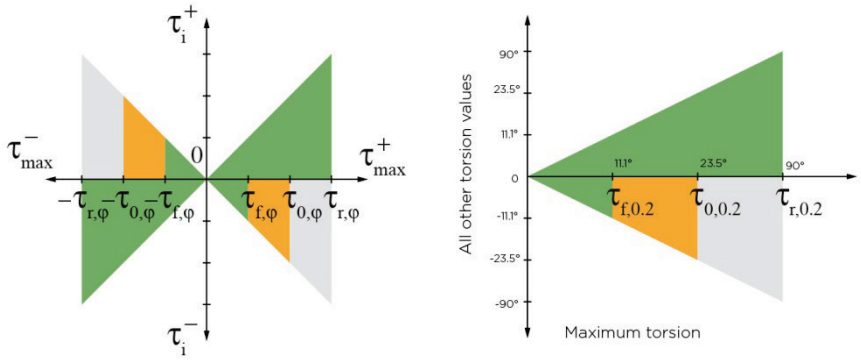

Figure 13. Horizontal axis shows the maximum value (τ_{max}) in tuple. Vertical axis shows the range $[\tau_i^-, \tau_i^+]$ for other torsion values around a node, which are smaller than or equal to the maximum value. The green area shows the collision-free solution space. The orange area designates the solutions space, where the drectionality of the torsion angles is important to avoid collisions, and the gray area shows torsion combinations, which always cause collison. Constants ($\tau_{f,\varphi}, \tau_{0,\varphi}, \tau_{r,\varphi}$) depend on (φ) and respectivly denote the (f) collision free zone, (0) boundary, where all torsion values have to have the same sign and (r) and operational limit for torsion combinations that can be achieved without collisions.

We saw above that there is a certain solution space in the orange zones of Figure 13, where collisions may or may not occur, depending on the directionality of torsion in diffferent edges around a node. We shall now look closer at the relationship between these torsion directionalities in order to identify patterns that create collision-free solutions better than others. As mentioned above, spiral configurations, where all edges are torsioned in the same direction, allow large degrees of torsion with no collisions. It is useful to know this spiral effect, but it has practical applicability as a fix to collisions in real-world structures. It is not possible to use sprialling nodes, for instance, in continuous tesselations with node degrees 5 and 6 , as shown in Figure 15. Generally, the spiralling solutions is limited to local fixes if the tesselation has an uneven number of edges around each loop or face.

The most collision-prone patterns we found invlovle torsion combinations where adjacent panels fluctuate between positive and negative torsion degrees, as illustrated in Figure 14. The figure shows how collisions are less likely when poitive and negative torsion values are arranged in sucessive edge groups and more likely when positive and negatives alternate from one edge to the next. The worst-case pattern for collisions occurs when edge torsions alternate with extreme values on neighboring edges: $[\cdots \tau_{max}, -\tau_{max}, \tau_{max,} -\tau_{max} \cdots]$.

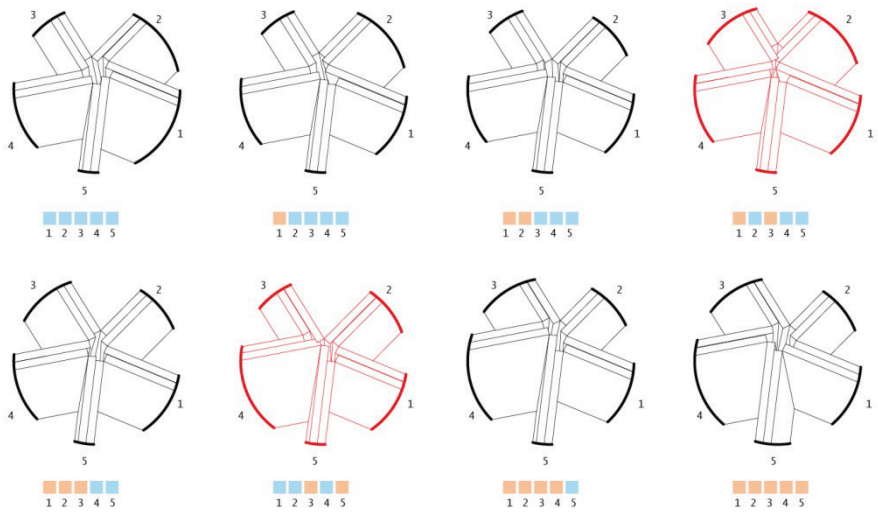

Figure 14. All possible combinations using necklace combinatorics for node degree 5. Blue indicates negative τ and orange positive τ values for indiviudal edges. Red diagrams denote cases where panel collisions occur.

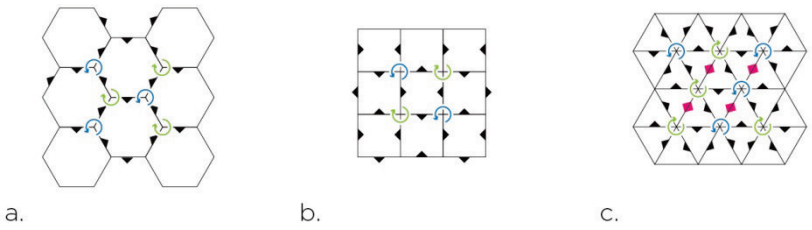

Figure 15. Regular hexagonal (a), quadrangular (b) and triangular (c) tessellations and the potential use of spiralling torsion at nodes to avoid collisions. Black arrows indicate the torsion direction in which an edge is leaning from a top view. Green and blue rotational arrows show the direction of spirals. Pink double arrows indicate edges, which have conflicting leaning directions.

2.1 Collisions caused by angles and curvature

The exploration of solution space for the double-walled grid structures showed that edge torsion was the greatest potential cause for panel collisions (see diagram in Figure 6). Without torsion, edge angularity and curvature around a node do not produce any collisions alone. But edge angularity and curvature could still deteriorate or ameliorate the collision space if combined with torsion.

To test the effects of edge angles on nodes whose edges already have torsion, we created a dataset with a node-degree 4, which has the following parameters:

$\tau_{max} = (2.8°, 2.5°, 2.0°, 1.5°, 1.0°)$, $\varphi = 0.05$ and altered the rotational angles of edges at one-degree intervals (Figure 16). We set a constant edge rotation angle α, which increases from $1°, 2°$ up to $20°$ on the vertical axis and tested rotations in each of the four edges around the node in a positive or negative direction according to the given rotation angle α. In the first column $\tau_{max} = 2.8°$ there are six distinct sub-columns, where the blue and orange colors denote all possible rotation directions with the given angle α: blue squares indicate edges that were rotated in the negative direction using α and orange squares indicate edges that were rotated in the positive direction using α. The six sub-columns under each τ_{max} value exhaust all possible rotational combinations for four edges. For all of these tests, we used the worst torsion pattern, where panels have alternating strongly negative and strongly positive torsion angles $[\tau_{max}, -\tau_{max}, \tau_{max,}, -\tau_{max}]$ (as shown in the last blue and orange column marked $\tau_{pattern}$ in the far right). The red and gray boxes show results, indicating whether collisions occurred (red) or not (gray).

These test results show that it does matter, which directional pattern the edge angles follow (see the blue and orange patterns under each column in Figure 16). As with torsion, most collisions occur if neighboring edges alternate between negative and positive angles. If all four edges have the same rotation angle in the same direction, then the whole node rotates without affecting the collision space (left most and right most cells in each column are gray, indicating no collisions). If the four edges are rotated in different directions, then collision in $\tau_{f,\varphi}$ are indeed affected. Depending on the angular direction pattern, collisions occur more frequently for edges with alternating angle directions than grouped angle directions.

But the findings also allow us to detect the solution space where angular rotations create no collisions at all despite the presence of torsion. The second column in Figure 16 illustrates that a four-edge node with very thin panels (small thickness-to-height ratio) $\tau_{f,0.05} = 2.5°$ can contain edge rotation angles up to -8° and 8° and stay collision free as long as these rotation angles are not alternating between each neighboring edge, but rather grouped sequentially by the direction of the rotation. For instance, both angular sequences (-8°,-8°, 8°,8°) and (-8°,8°, 8°,8°) are collision free even under the worst alternating torsion pattern.

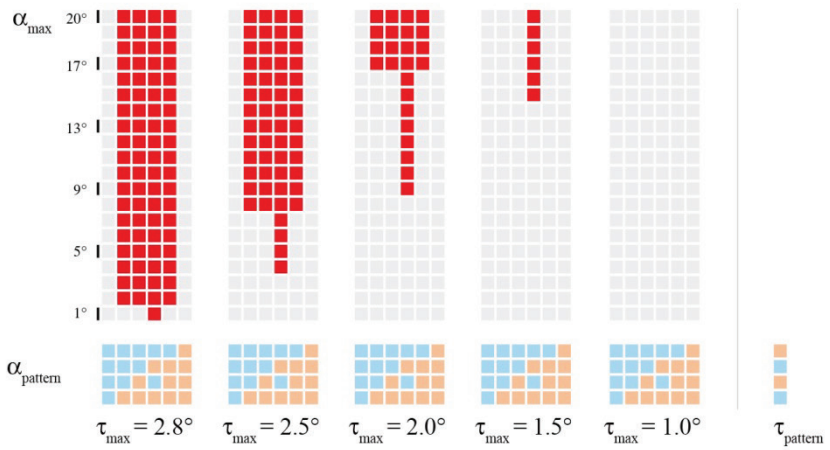

Figure 16. Bottom part of the diagram shows patterns used for angles. Blue boxes indicate negaitve and orange positive angle directions. Far right column indicates the torsion directionality pattern. Every column simulates one torsion value for six different combinations of panel angle degrees, which are repeated for each degree from 1° to 20°. Red squares denote cobinations with collisions, gray with no collisions.

Finally, we also performed similar studies on the effects of curvature (Figure 5), but found somewhat surprisingly that curvature has no effect on collisions produced by edge torsion. This is logical at a second glance, since curvature does not affect loop-node vectors $v_{l,n}$ and therefor also does not create any additional collisions (see Figure 6).

Conclusions

The paper has investigated a new method for realizing grid structures, which relies on double walls along each network edge. A double-walled nature enables us to significantly reduce the geometric complexity of the grid structure's nodes – instead of needing to find a combined geometric intersection for all edges meeting at a node, our solution instead requires determining a pair of adjacent planes at a time, as many times as a node's degree.

The key benefit of this method is that it makes grid structures possible on a wide variety of curved surfaces and on a large selection of line-network patterns with relatively simple geometric operations. The entire structure can be made out of planar components that are fabricated only using two-dimensional cutters, such as laser-cutters, blade-cutters, 3-axis routers, etc., making the fabrication significantly cheaper than traditional grid structures.

While the method is fairly robust and flexible with thicker panels (or thinner panels with spacer blocks between them), collisions can occur between edges around a node when panels are thin or the geometries of the nodes complex. Such collisions can prevent the realization of the structure due to joints that do not fit. It

was therefore important to investigate the solution space that exists for such structures without any collisions under different geometrical and material parameters.

First, we found that the easiest solution to avoiding panel collisions around nodes involves adding thickness to the panels (or placing spacer blocks between parallel panels). This simple move can make relatively complex structural geometries collision free (Figure 17). But this fix is not always applicable – for either engineering or aesthetic reasons, small thickness-to-height ratios may be important or desirable for a structure.

Second, we found that panel collisions around nodes are almost entirely caused by torsion in the edges. The angles and curvature of intersecting edges alone had no effect on collisions, they mattered only in conjunction with torsional panels. The paper thus mainly investigated the effects of torsion on collisions. We found the following.

The maximum magnitude of torsion observed among all edges converging on a node has a significant effect on collisions. The absolute value of the most torsioned edge $|\tau|_{max} = \max(|\tau_1|, \cdots |\tau_i|, \cdots |\tau_e|)$ in t_n can alone predict whether or not collisions occur. If the highest torsion angle does not create collision, then none of the lower torsion angles in edges around the same node $|\tau_{i \in t_n}| < |\tau|_{\max}$ produce collision.

A maximal collision-free torsion magnitude $|\tau|_{\mathrm{m}}$ for a node of degree $d_n = i$ applies very similarly to any other node degree $d_n \in [4, \mathbb{I}]$. This means that if we find a collision-free torsion limit for a node with four edges ($d_n = 4$), then we can use the same limit for $d_n = 6$ and so on. This works because the first collision occurs with the first adjacent edge each time.

There are three distinct zones in the collision-free solution space for torsion values under all material thickness-to-height ratios. First, smaller values under $\tau_{f,\varphi}$, which can contain any combination and direction of torsioned panels until the limiting torsion angle $\tau_{f,\varphi}$. Second, large torsion values above $\tau_{0,\varphi}$ where panels around a node must all be torsioned as a spiral in the same direction (either negative or positive direction). And third, collision-free solutions can also be found with intermediary torsion angles between $\tau_{f,\varphi}$ and $\tau_{0,\varphi}$ where the pattern of torsion directionality becomes decisive for collisions. For instance, an alternating patter of maximum torsion - minimum torsion - maximum torsion between adjacent edges around a node is most collision prone, but if the edges with the same torsion direction are grouped next to each other, collisions can be avoided. Particular numeric limits for allowable torsions angles for each material thickness-to-height ratio were determined as part of the tests.

These findings make it possible to detect potential collisions at a grid-structure's nodes computationally, using the torsion, angle, curvature and material thickness-to-height ratios. Furthermore, the findings can also help solve these collisions computationally, by adjusting the edge geometries around each node such that all nodes fall in the solution space. Whereas we have so far produced a RhinoPython library for generating the above grid-structures, it will remain a research and development task for the future to include automated collision detections and collision fixes in the library.

The presented method of grid structure generation was used to build an experimental pavilion at the Singapore University of Technology and Design (Figure 17). At the time of construction, the intricacies of the geometric solution spaces were not known to us. As a result, we relied heavily on increasing the gap size between panels in order to avoid collisions at nodes. The new findings can enable analogous structures to be created out of very thin panels with no gaps between them.

Figure 17. Completed SUTD gridshell project by the SUTD City Form Lab and ARUP engineering.

References

MUNGAN, I., ABEL, J. 2012 *Toward Lightness In Concrete: Some 20th Century Shells and Bridges*. Journal of the International Association for Shell and Spatial Structures (J. IASS). Vol. 5

PÓLYA, G. 1937. *Kombinatorische Anzahlbestimmungen für Gruppen, Graphen und chemische Verbindungen*. Acta Mathematica 68 (1): 145–254.

PRONK, A., DIMINICUS, M., 2013. *84 ways to Manipulate a Membrane*. Journal of the International Association for Shell and Spatial Structures, 612: 257 – 270

SCHLAICH, J. 2002, O*n Some Recent Lightweight Structures*, Journal of the International Association for Shell and Spatial Structures (J. IASS). Vol. 43 (2002) No. 2 August n. 139

SCHNEIDER, P., EBERLY, D 2003. *Geometric Tools for Computer Graphics.* Morgan Kaufmann Publishers. 14-15

SEVTSUK A., KALVO, R. 2014 *A Freeform Surface Fabrication Method with 2D Cutting*. SimAud 2014 proceedings. 109 – 116.

WELLS, D. 1991. *The Penguin Dictionary of Curious and Interesting Geometry.* Penguin. 121, 213, and 226-227.

Authors' address:

Andres Sevtsuk (andres_sevtsuk@sutd.edu.sg)
Singapore University of Tehcnology and Desing
20 Dover Drive, 138682, Singapore

Raul Kalvo (raul_kalvo@sutd.edu.sg)
Singapore University of Tehcnology and Desing
20 Dover Drive, 138682, Singapore